

**Flight kinematics of the barn swallow (*Hirundo rustica*) over a  
wide range of speeds in a windtunnel**

Kirsty J. Park<sup>1</sup>, Mikael Rosén<sup>2</sup> & Anders Hedenström<sup>2</sup>

<sup>1</sup>Department of Biological Sciences, University of Stirling, Stirling FK9 4LA

<sup>2</sup>Department of Animal Ecology, Lund University, SE-223 62 Lund, Sweden

<sup>1</sup>Author for correspondence KJ Park

Tel. (01786) 467799

Fax (01786) 464994

E-mail: k.j.park@stir.ac.uk

## Summary

Two barn swallows (*Hirundo rustica*) flying in the Lund wind tunnel were filmed using synchronised high-speed cameras to obtain posterior, ventral and lateral views of the birds in horizontal flapping flight. We investigated wingbeat kinematics, body tilt angle, tail spread and angle of attack at speeds of 4 to 14 ms<sup>-1</sup>. Wingbeat frequency showed a clear U-shaped relationship with air speed with minima at 8.9 ms<sup>-1</sup> (bird #1) and 8.7 ms<sup>-1</sup> (bird #2). A method previously used by other authors of estimating the body drag coefficient ( $C_{D,par}$ ) by obtaining agreement between the calculated minimum power ( $V_{min}$ ) and the observed minimum wingbeat frequency does not appear to be valid in this species, possibly due to upstroke pauses that occur at intermediate and high speeds, causing the apparent wingbeat frequency to be lower. These upstroke pauses represent flap-gliding, possibly a way of adjusting the force generated to the requirements at medium and high speeds, similar to the flap-bound mode of flight in other species. Body tilt angle, tail spread and angle of attack all increase with decreasing speed, thereby providing an additional lift surface and suggesting an important aerodynamic function for the tail at low speeds in forward flight. Results from this study indicate the high plasticity in the wing beat kinematics and use of the tail that birds have available to them in order to adjust the lift and power output required for flight.

## Introduction

During horizontal powered flight, a bird must flap its wings to generate lift and thrust to overcome gravity and drag. The instantaneous forces on the wings vary during the course of a wingbeat cycle due to time-varying wing planform, degree of flexing the elbow and wrist joints, angle of attack, wing twist, rotational velocity of wings, elastic properties of the primaries, forward velocity, etc. The kinematics of a wingbeat is dynamically a very complicated process, yet it contains the physical key to the mechanical power required to fly, and hence is of interest to researchers.

Depending on species, i.e. size and morphology, birds will flap their wings continuously or in bursts with wingbeats interspersed by phases of glides or bounds, the latter flight mode resulting in a sinusoidal flight trajectory around the horizontal level. Species using bounding flight or intermittent flight (wings not completely folded during the non-flapping phase) include the budgerigar *Melopsittacus undulatus*, finches such as the zebra finch *Taenopygia guttata*, starling *Sturnus vulgaris* and woodpeckers (Rayner, 1995; Tobalske, 1995, 1996; Tobalske and Dial, 1994; Tobalske *et al.*, 1999). In birds that typically use continuous flapping flight, some characteristics of the wingbeat kinematics change with speed. For example, in some species the relation between wingbeat frequency and speed is U-shaped (Pennycuick *et al.*, 1996), in a similar way to the mechanical power output of bird flight (Pennycuick, 1975, 1989a; Rayner 1979, 1999). In other species, such as the starling, wingbeat frequency appears to have a more or less linear relationship with air speed (Tobalske, 1995), or there is no systematic change with speed (black-billed magpies, *Pica pica* and pigeons, *Columba livia*: Tobalske and Dial, 1996). Other features of wingbeat kinematics related to force generation may also change in relation to forward air speed.

Birds' tails also play an important aerodynamic role in mechanical flight power and flight performance. Conventional models of bird flight ignore the tail (e.g

Pennycuick,1989a), although it has been calculated that the tail of many birds could generate as much as a third of the total lift required to support a bird's weight (Thomas, 1995).

In this paper we present data on wing and tail kinematics over a wide range of speeds in two swallows *Hirundo rustica* flying in a wind tunnel. We observed interesting features associated with flapping flight and we discuss these findings in relation to the theory of flight mechanics.

## **Materials and methods**

### **Windtunnel**

The experiment was conducted in a low-turbulence, closed-circuit design wind tunnel at Lund University, Sweden (for design details see Pennycuick *et al.*, 1997). The test section is octagonal in cross section and is 1.22 m wide by 1.08 m high. The first 1.20 m length of the test section is enclosed by Plexiglas walls, and the last 0.5 m is open, giving unrestricted access to the bird. A pitot-static survey showed that the air speed was within  $\pm 1.3\%$  of the mean across 97.5% of the test section, only deviating from this value at 3 corner points, while hot-wire anemometer measurements showed that the turbulence in the closed part of the test section was as low as 0.04 % of the wind speed (Pennycuick *et al.*, 1997). A fine nylon net of thread diameter 0.15 mm, with a mesh size of 29mm $\times$ 29mm, was placed across the exit from the contraction about 50 cm upstream from the position of the bird in the test section. This net will introduce a small additional turbulence into the flow (Pennycuick *et al.*, 2000).

### *Equivalent air speed*

The Lund windtunnel uses dynamic pressure ( $q$ ) to set the equivalent air speed ( $V_e$ ) which can be defined as

$$V_e = \sqrt{(2q/\rho_0)},$$

where  $\rho_0$  is the value assumed for the air density ( $1.23 \text{ kg m}^{-3}$ ) at sea level under International Standard Atmospheric conditions. The disparity between true and equivalent air speed varies depending on changes in air temperature and barometric pressure. Equivalent air speed is used throughout this paper, as it is this that determines the magnitudes of aerodynamic forces acting upon the bird.

### *Birds and training*

Four adult male barn swallows were caught near Lund, Sweden, on May 21 1999. All were willing to fly in the windtunnel from the beginning but two birds flew more steadily and for longer periods than the others and were therefore chosen for the experiment (for morphological details see Table 1). Over the first week each of the birds was trained to fly in the windtunnel for approximately 1 hour per day. After this the two birds used in this experiment were sufficiently steady in flight (maintaining their position in the horizontal and vertical planes) for data collection. All birds were released at the original capture site after the experiment was completed on June 16, 1999.

### *Kinematic analysis*

Swallows were filmed while flying in the windtunnel using two high speed RedLake video cameras (Motionscope PCI 500, USA) at  $125 \text{ frames s}^{-1}$  and with the shutter open for  $1/1875$  seconds. The cameras were synchronised to record simultaneous images of the bird from different angles. The camera output was directly transferred via frame grabbers to a PC (Pentium II 233 MHz) in the form of two animation (.AVI) files, one from each camera. Then individual frames were extracted from these files as sequences of compressed (.JPG) monochrome picture files, measuring  $480 \text{ pixels} \times 420 \text{ pixels}$ , where pixels were square

(aspect ratio 1). Flight sequences, averaging 1.3 s in duration, of posterior (image plane x, z) and ventral (image plane y, z) views of the swallows were obtained by positioning one camera behind the test section far back in the first diffuser without affecting the flow in the test section (see Pennycuick *et al.* 1997), and the other underneath the test section. The coordinate axes are defined as: x = direction of flow, y = vertical direction, and z = perpendicular to x and y. The distance of the ventral view camera to the bird was about 70 cm, while the posterior view camera was placed 3 m behind the bird. Swallows were filmed in steady flight at 1ms<sup>-1</sup> intervals between 4 and 14 ms<sup>-1</sup>. Air speeds were set randomly and five flight sequences obtained for each air speed. One bird (#2) would not fly at 14 ms<sup>-1</sup> so the top air speed for this bird is 13 ms<sup>-1</sup>. After five flight sequences at each air speed had been obtained for posterior and ventral views, one of the cameras was moved to the side of the test section and lateral views of swallows were filmed to obtain body and tail tilt angles. Again, five replicate flight sequences containing one full wingbeat were obtained for each air speed. Film analysis was carried out using Redlake Imaging Motionscope 2.16, allowing pixels to be marked and reading of current pixel co-ordinates, which allowed the calculation of angles between lines. Wing areas were measured in Mapinfo Professional 4.5 by using the reference length on the bird (REF, see Table 1). The following data were extracted from the posterior, ventral and lateral views of the swallows in flight:

- 1) Wingbeat frequency was calculated by dividing the number of wingbeats by the number of frames and converting the value to wingbeats s<sup>-1</sup> (Hz). To calculate the wingbeat cycle period the inverse of wingbeat frequency was taken.

- 2) Wingbeat amplitude was calculated as the angle described by the pivoting of the right shoulder joint-wrist line during the time between the end of an upstroke and the end of the next downstroke (see Pennycuick *et al.* 2000). The shoulder joint was a well defined point easily distinguished on the posterior view images. Wingbeat amplitude using the shoulder

joint-wingtip line was also calculated for direct comparison with other studies. The beginning or end of a stroke was defined as the point where the wing amplitude angle reached maximum values above or below the horizontal in the xz plane. Ensuring that the bird was in horizontal flight, a maximum of ten wingbeat amplitudes from the right wing was calculated for each flight sequence (range 1-10) and the average taken. From these data, the duration of the downstroke and its angular velocity, and the up and downstroke fractions of the wingbeat cycle period were also calculated. Downstroke angular velocity was calculated by converting the duration of the entire downstroke in frames, to seconds and calculating velocity as radians per second. Due to the 8 ms per frame as the minimum time resolution for any instantaneous kinematic event, the maximum error of stroke duration was 16 ms, which is about 20 % of the maximum downstroke duration. Note that on average the error will be 8 ms for determining stroke duration, which is half that of the maximum.

3) Wingspan: For each speed the lengths of the mid-downstroke and mid-upstroke wingspan (wingtip to wingtip) were measured and the span ratio expressed as the upstroke span divided by the downstroke span. Lengths were obtained using Mapinfo and a reference length of a known distance on the bird was used to calibrate the values (see Table 1). Three downstroke and upstroke spans were calculated and averaged for each flight sequence.

4) Upstroke pauses: It was observed that in steady level flight swallows would occasionally pause for a fraction of a second in the middle of the upstroke. The duration of these pauses were measured and averaged per wingbeat with pauses across the entire flight sequence. Not all wingbeats exhibited such pauses and so we also noted the proportion of wingbeats with upstroke pauses. Due to the frame frequency (125 Hz) of the cameras, the minimum pause length that could be detected was if the wing remained in the same position on two consecutive frames, representing a minimum time of 8 ms. Our measurements hence underestimate the duration of the pauses by a maximum 16 ms and on average 8 ms.

5) Body tilt angle was calculated from lateral flight sequences by drawing a line between the sharp angle of the inner dorsal bill and the feathering and the tip of the central tail feather, and measuring the angle of the line relative to the direction of airflow, given by the metal frame of the tunnel test section. Body tilt angles at the end of the downstroke, mid-upstroke, and the end of the upstroke were calculated and averaged for each flight sequence.

6) Tail spread angle and angle of attack were calculated from ventral and lateral flight sequences respectively. Tail spread angle was calculated by drawing two lines out from the centre of the tail (where it meets the body) to the tips of the tail streamers. Care was taken to use only those images where the bird was in steady forward flight (not moving side to side) and the streamers were straight-sided. Three tail spread angles at mid-downstroke were measured and averaged for each flight sequence. Tail angle of attack was measured in a similar way to body tilt, measuring the angle of the line between the proximal and distal ends of the central tail feathers to the direction of airflow. One measurement at mid-downstroke was made for each flight sequence.

### *Statistics*

Analyses were carried out using General Linear Models in MINITAB release 12.1 (Ryan *et al.* 1985). Mean values were calculated for the flight variables at each airspeed. A model was constructed for each of the flight variables (dependent variable) with airspeed (covariate) included initially as a linear, quadratic, and upto quartic term, then sequentially removing the highest level non-significant terms. Residuals from the analyses were tested for normality (Anderson-Darling) and homoscedascity, and descriptive data are presented as means  $\pm$  s.e. The bootstrapping procedure was carried out using S-PLUS 4.5 (MathSoft Inc. 2000).

### **Results**

The lowest air speed at which the swallows were consistently able to maintain forward flapping flight was  $4 \text{ ms}^{-1}$ , although one swallow did fly briefly at  $3.4 \text{ ms}^{-1}$ . At air speeds lower than this the birds would adopt turning flight before settling onto the base or sloping sides of the test section. The highest speeds we were able to obtain film sequences for was at  $14 \text{ ms}^{-1}$  (bird #1) or  $13 \text{ ms}^{-1}$  (bird #2). At air speeds higher than this the birds would fly for very short periods of time, but typically would hold on to the net at the back of the test section and appeared unable to maintain sufficient flight speed.

Data are presented graphically for the two swallows separately, with swallow #1 indicated by (i) after the figure letter, and swallow #2 by (ii). Statistics are given in the figure legends, and equations for the fitted lines are provided in Table 2.

#### *Wingbeat kinematics*

Wingbeat frequency ranged from 6.95 to 8.99 Hz in bird #1, and 7.07 to 8.42 Hz in bird #2 and, for both birds, showed a curvilinear relationship with air speed (Fig. 1). The quadratic function of the relationship was derived from the regression coefficients, and differentiated to find the minima (wingbeat frequency versus air speed). Bootstrapping was used to generate a population of minima from the original data set allowing 95% confidence intervals to be estimated. Minimum wingbeat frequency speed for bird #1 was  $8.89 \text{ ms}^{-1}$  (95% confidence intervals: 7.88 - 9.90), and for bird #2 it was  $8.66 \text{ ms}^{-1}$  (8.00 - 10.00). The corresponding wingbeat frequencies at these speeds were 7.04 Hz (6.62 - 7.50) for bird #1, and 7.11 Hz (6.67 - 7.51) for bird #2.

The wingbeat cycle period, i.e. the duration of a downstroke and upstroke, was divided into upstroke and downstroke fractions. The downstroke fraction decreased from near 0.50 at  $4 \text{ ms}^{-1}$  to 0.40 at  $14 \text{ ms}^{-1}$  in bird #1 (Fig. 2). Bird #2 showed higher values with a similar

decrease with air speed from 0.54 at 4 ms<sup>-1</sup> to 0.45 at 12 ms<sup>-1</sup>, but with a somewhat higher value at 13 ms<sup>-1</sup>.

Wingbeat amplitude increased with air speed (Fig. 3A) from approximately 70° at low speeds to over 120° at high speeds. Wingbeat amplitude on the basis of wingtip movements yielded consistently about 10° higher values than shoulder joint-wrist amplitude (Fig. 3A), indicating that the wing bends at the wrist at the bottom of the downstroke. The duration of the downstroke increased between 4 ms<sup>-1</sup> and 7 ms<sup>-1</sup> and then decreased with increasing air speed (Fig. 3B i). This pattern was more apparent in bird #1 than bird #2, which showed a peak in downstroke duration at 5 ms<sup>-1</sup> (Fig. 3B ii). The angular velocity of the downstroke remained fairly constant at low speeds until an air speed of approximately 7 ms<sup>-1</sup> was reached after which angular velocity increased with air speed (Fig. 3C).

Wingspan was maximal at mid-downstroke and minimal during mid-upstroke. Mid-downstroke wingspan decreases with increasing air speed from approximately 32cm at 4ms<sup>-1</sup> to between 26cm (bird #1) and 29cm (bird #2) at the highest air speeds (Fig. 4A). Mid-upstroke wingspan and span ratio increased from 4 ms<sup>-1</sup> to maximum values at 5 ms<sup>-1</sup>. Both measures then showed a gradual and near linear decline with further increasing air speed until approximately 10-11 ms<sup>-1</sup>, after which wingspan and span ratio showed little change (Fig. 4B,C).

A pause during the upstroke of the wingbeat cycle was only observed at air speeds exceeding 8 ms<sup>-1</sup> for bird #1, and 5 ms<sup>-1</sup> for bird #2. At these speeds, upstroke pauses (8 to 56 ms duration) did not always occur during every wingbeat cycle but would often skip a few wingbeats and then resume. Runs of wingbeats with upstroke pauses typically varied between 1 and 3, with maximum 6 consecutive wingbeats containing pauses. Both birds showed an initial increase in the duration of the upstroke pause up to an average at about 20 ms at 10ms<sup>-1</sup> (Fig. 5). The proportion of wingbeats with an upstroke pause was maximum at 61% at 12

$\text{ms}^{-1}$  for bird#1, and 69% at  $11 \text{ ms}^{-1}$  for bird#2, with lower proportions below and above these speeds. The position of the wings during the pause was identical to that during mid-upstroke of wingbeats without a pause. Hence, during a pause the wings were held in a position so that some lift (and drag) was generated. The wing tip showed an elliptical trajectory at speeds of 4, 8 and  $12 \text{ ms}^{-1}$  when viewed laterally, with the wingtip more anterior during downstroke than during upstroke (Fig. 6A). The path of the wingtip moved back along the horizontal axis of the bird with increasing speed, reflecting the fact that the wing was increasingly flexed at higher air speeds. From a rear view the wingtips also traced an elliptical trajectory, with a more distally position of the wingtip during the downstroke than during the upstroke (Fig. 6B). At  $12 \text{ ms}^{-1}$ , the illustrated example indicates the position and duration of an upstroke pause as observed (Fig. 6).

#### *Body tilt, tail spread and tail angle of attack*

Body tilt angle ranged from  $5$  to  $21^\circ$  from horizontal, decreasing with increasing air speed (Fig. 7). Changes in air speed from  $4$  to  $6 \text{ ms}^{-1}$  caused marked reductions of approximately 40% in body tilt angle. Once air speeds of  $11$ - $12 \text{ ms}^{-1}$  had been reached, body tilt angle remained fairly constant at between approximately  $5$  and  $8^\circ$ . The angle of tail spread at very low air speeds reached a maximum of  $56.6^\circ$  (bird #2) at  $4 \text{ ms}^{-1}$  although the average tail spread angle at this speed was considerably lower (Fig. 8A). For both birds tail spread angle decreased with increasing air speed until  $7$ - $8 \text{ ms}^{-1}$ , whereupon it became relatively constant at approximately  $6.4^\circ$  for bird #1 and  $8.4^\circ$  for bird #2. The angle of attack of the tail to the direction of airflow also decreased with increasing air speed, from  $20$ - $25^\circ$  at  $4 \text{ ms}^{-1}$  to  $1$ - $5^\circ$  at  $12$ - $14 \text{ ms}^{-1}$  (Fig. 8B). At the lowest air speeds, tail angle of attack exceeded the body tilt angle, whereas at air speeds higher than  $6 \text{ ms}^{-1}$ , body tilt was greater than that of the tail.

#### *Estimating body drag coefficient*

Pennycuick *et al.* (1996) assumed that speeds of minimum power and minimum wingbeat frequency are identical and used this assumption to indirectly estimate the body drag coefficient. They used the flight mechanical theory of Pennycuick (1989a), from which it is possible to calculate mechanical power required for flight and characteristic flight speeds such as the minimum power speed ( $V_{mp}$ ). By changing the body drag coefficient,  $C_{D,par}$ , the mechanical power as calculated by the program will change and hence also  $V_{mp}$  equal to the observed speed of minimum wingbeat frequency. Using this method we obtained a  $C_{D,par}=0.03$  for both birds using the estimated speeds of minimum wingbeat frequency (see above).

## **Discussion**

The patterns of wingbeat kinematics observed were strikingly similar in the two barn swallows studied, suggesting that our results are general to barn swallows. The function of the tail streamer in the barn swallow is a subject of much debate (Norberg, 1994; Barbosa and Møller, 1999; Evans, 1998, 1999; Hedenström and Møller, 1999; Buchanan and Evans, 2000), and aerodynamic modelling has been employed to investigate the possible effect of tail streamers on flight (Evans and Thomas, 1992; Thomas, 1993). However, wing kinematics and aerodynamic performance of the swallow as a whole, has to date, been largely ignored. In horizontal flight, our study subjects flew readily from  $4 \text{ ms}^{-1}$  to  $13\text{-}14 \text{ ms}^{-1}$ , with steady flight for brief periods ( $< 20$  seconds) at a maximum  $15 \text{ ms}^{-1}$ . Above about  $7 \text{ ms}^{-1}$ , the tail was furled and the drag from the tail streamers would have been negligible. The area of two tail streamers beyond the trailing edge of the tail is approximately  $150 \text{ mm}^2$  in a barn swallow, which is only about 0.9 % of the total projected area of the bird. At lower speeds and during turning, the tail was spread and tail angle of attack exceeded that of body tilt, probably increasing the lift to drag ratio of the whole bird (Thomas, 1993). Our results

indicate that the tail as a whole probably has an aerodynamic function at low speed and may provide an additional lifting surface.

### *Wingbeat frequency and body drag*

The range of wingbeat frequencies observed during this study (7-9 Hz) corresponds closely to the 8.2 Hz calculated by Pennycuick using a formula based on a barn swallows' size and morphology (Pennycuick, 1996). Danielsen (1988) measured 9.0 and 9.3 Hz in two barn swallows on migration, i.e showing similar wingbeat frequency as our swallows when flying in the higher speed range. Compared with other species of similar size, the swallow has quite low wingbeat frequency and relatively long wings that increase the wing moment of inertia. Wingbeat frequency showed a clear U-shaped relationship with air speed with minima at  $8.9 \text{ ms}^{-1}$  and  $8.7 \text{ ms}^{-1}$  for bird #1 and bird #2, respectively. A measure of the drag caused by the body (body drag coefficient,  $C_{D,\text{par}}$ ) is required to calculate the mechanical power of flight in relation to air speed in birds (Pennycuick, 1989a). The speed of minimum wingbeat frequency is believed to be identical with the speed associated with minimum power ( $V_{\text{mp}}$ ) (e.g. Pennycuick *et al.* 1996). Agreement between calculated  $V_{\text{mp}}$  (using  $C_{D,\text{par}}$ ) and observed wingbeat frequency can be obtained by adjusting the value of  $C_{D,\text{par}}$ , allowing a more "realistic" estimate of  $C_{D,\text{par}}$  to be calculated. Pennycuick *et al.* (1996) found that, to get a match between calculated  $V_{\text{mp}}$  and minimum wingbeat frequency in a thrush nightingale and a teal, the  $C_{D,\text{par}}$  had to be set at 0.08 rather than the "old default" value of 0.4 (cf. Pennycuick, 1989a). Using the same technique for the two swallows we found that  $C_{D,\text{par}}$  must be reduced even more to 0.03. However, if we consider the plots of wingbeat frequency in relation to speed (Fig. 1), one will note two minima, at  $7\text{-}8 \text{ ms}^{-1}$  and  $10 \text{ ms}^{-1}$ , with slightly elevated values in-between. This pattern is present in both birds and can be attributed to the upstroke pauses observed at speeds above about  $7\text{-}9 \text{ ms}^{-1}$ , which causes the apparent

wingbeat frequency to decline and shift the speed of minimum wingbeat frequency upwards. Hence, the continuous flapping flight speed of minimum wingbeat frequency should be lower, and closer to the speed of minimum power than the apparent values estimated from Fig. 1. Hence, if instead using the lower ends of the 95% confidence limits around the estimated minima for speeds of minimum wingbeat frequency (7.88 and 8.00 ms<sup>-1</sup> for bird#1 and bird#2, respectively), we get  $C_{D,par}$  = 0.05 and 0.04 for the two birds, respectively. Although swallows are streamlined birds these values seem extremely low.

Pennycuick *et al.* (2000) developed a new technique for directly estimating the mechanical power required to fly in birds. This method is based on the observation that the birds' body exhibits vertical movements, such that it raises its position in relation to the horizontal during the downstroke, when most of the lift force is generated, and lowers its position during the upstroke. By measuring the amplitude of the humeral excursion and angular velocity of the wings, Pennycuick *et al.* (2000) were able to calculate the mechanical power output of a swallow (swallow #1 of this study). The mechanical power was only calculated for speeds of 6-11 ms<sup>-1</sup>;  $C_{D,par}$  was set to 0.26 and the profile power ratio  $X_1$  to 2.25. These values achieved the best fit between calculations of the mechanical power using the body drag coefficient and profile power ratio (Pennycuick 1989a) and the average mechanical power derived from wind tunnel observations (see Pennycuick *et al.*, 2000 for details). The  $V_{mp}$  was estimated at 5.3 ms<sup>-1</sup> for this swallow and these parameter settings, which is clearly outside the 95% confidence interval for the speed of minimum wingbeat frequency (7.9-9.9 ms<sup>-1</sup>, see Results). Estimating  $C_{D,par}$  on the basis of wingbeat frequency, therefore, may not be valid in this species.

### *Flight mode and kinematics of wings and tail*

Many smaller bird species exhibit bounding or intermittent flight in which bursts of wingbeats are followed by periods without wingbeats (e.g. Rayner, 1985; Tobalske *et al.*, 1999). There are two main explanations for the function of bounding flight: the first postulates that the total drag taken over an entire bounding cycle is lower than had the bird flapped its wings continuously because the profile drag is reduced by folding the wings for a fraction of the cycle (Lighthill, 1977). The second explanation, the “fixed-gear hypothesis”, assumes that the fibres of the pectoralis muscle restrict small birds to a narrow range of frequencies where the efficiency of the muscle is maximum (Rayner, 1985). This second hypothesis implies that bounding is a means of adjusting the power output to the level required for a certain flight speed. In zebra finches the wingbeat frequency increased from 25 Hz at 0 ms<sup>-1</sup> (hovering) to 27 Hz at 14 ms<sup>-1</sup> (Tobalske *et al.* 1999), a 12% increase compared with the 19% and 29% increase from minimum to maximum wingbeat frequency in the two swallows. It is possible that differences in the relative ranges of wingbeat frequencies used over the same range of speeds in zebra finch and barn swallow represent the variation between a typical bounding species using continuous flapping and flap-gliding. The upstroke pauses seen in the swallows may be a way to adjust the force generation to the required level at medium and high speeds, and may perhaps be regarded intermittent flap-gliding (cf. Danielsen, 1988).

Amplitude increased with speed, which combined with downstroke duration yield a nearly constant downstroke angular velocity between 4-7 ms<sup>-1</sup>, which then increases with further increase in air speed. Changes of these parameters are closely linked to the force generation of the wings and the power output (cf. Pennycuick *et al.*, 2000). The wing-tip showed elliptical paths when viewed laterally, with the centre of the ellipse moving back along the horizontal axis of the bird with increasing airspeed. This is similar to that of

pigeons at speeds of  $10 \text{ ms}^{-1}$  and above, but not magpies which show no apparent differences in relation to speed (Tobalske and Dial, 1996). It is perhaps due to this that the pigeon and the swallow are more similar with respect to wing morphology than the swallow and magpie.

The reduction in the degree of body tilt and tail spread, with increasing speed is similar to that reported for magpies and pigeons by Tobalske and Dial (1996). In addition, our data show that the tail angle of attack exceeds body tilt at low air speeds, and decreases with increasing speed. These observations suggest that there is an aerodynamic function of the tail at low speeds. Thomas (1996) used a simple aerodynamic model to argue that the power required for flight at low speeds can be reduced by increasing both the degree of tail spread and the angle of attack. While there are broad similarities in the direction of change predicted by the model and that observed in this study, there are both qualitative and quantitative differences which indicate that modifications to the model are required (Evans, Rosén, Park and Hedenström, in prep.).

#### *Variable wing span*

Pennycuick (1989b) developed a method for calculating the lift:drag ratio based on the “span ratio”, i.e. the ratio of the wingspan during the upstroke to that during the downstroke, assuming that the circulation of the wingtip vortices and the lift distribution remains constant throughout the cycle. A concertina wake concomitant with these properties was observed in a kestrel *Falco tinnunculus* (Spedding, 1987). A requirement for applying the simplified span ratio method to calculate effective lift:drag ratios is that the duration of the up- and downstrokes are the same (Pennycuick, 1989b), which was obviously violated in our swallows (see Fig. 2). The span ratio declined with increasing speed from 0.5 at  $5 \text{ ms}^{-1}$  to about 0.2 or less at  $10\text{-}11 \text{ ms}^{-1}$ , but it was 0.4 at  $4 \text{ ms}^{-1}$ . The lower value at  $4 \text{ ms}^{-1}$  indicates that the upstroke is feathered at this speed and provides no lift, although the upstroke does

provide small lift forces at higher speeds ( $\geq 6 \text{ ms}^{-1}$ ) as indicated by the observations of vertical accelerations of the body (Pennycuik *et al.*, 2000). The swallow body accelerated downwards during the wing upstroke, although not as much as during a free fall, which is evidence for an upward lift force. An interesting observation regarding the span ratio was that the wingspan at mid-downstroke declined from the maximum possible at  $4 \text{ ms}^{-1}$  with a 3-5 cm reduction in wingspan at higher speeds. We did not observe any drastic changes in either the upstroke nor the downstroke kinematics, suggesting that the wingbeat kinematics change in a continuous manner in relation to air speed. Such changes of kinematics differ from those predicted by the “gait theory” of flapping forward flight, but as yet we have no data on the actual vortex wakes of these birds. The span during the upstroke declined even more than during the downstroke resulting in the overall decline in span ratio. Even if the span reduction during downstrokes was quite small, it may be analogous to the wingspan adjustments in gliding flight (Tucker, 1987). In gliding flight, reducing the span with increasing speed increases the overall lift:drag ratio of the bird, by trading profile drag against required lift production. We propose that by reducing the span at high speeds the swallow will reduce the profile drag and yet produce enough lift to overcome induced and parasite drag. This analogy does however not apply to Pennycuik’s (Pennycuik, 1989a) method of calculating the profile power as a multiple of the “absolute minimum power” – a quantity that is proportional to  $b^{-3/2}$ , where  $b$  is wingspan. Then profile power is always minimum with maximum wingspan and there is no trade-off with induced power. In pigeons and magpies, also studied in a windtunnel, the span during mid downstroke was constant across a wide speed range (Tobalske and Dial, 1996). Other bird species with high aspect ratio wings, such as arctic tern *Sterna paradisaea* and skuas *Stercorarius* spp., likewise flex their wings and reduce their wingspan during downstroke when observed in fast cruising or chasing flights (pers. obs.).

Depending on size and structure there are many ways that birds can adjust the lift and power output required in relation to speed, including changing wingbeat frequency, wingbeat amplitude, span and span ratio, body tilt angle, tail angle of attack, etc. Considering the plasticity in this system it may be inferred that some caution is warranted when equating speeds of minimum wingbeat frequency and minimum power (cf. Pennycuick *et al.*, 2000). There is a continuum with respect to flight kinematics between continuous flapping flight to bounding flight, including the intermittent flap-gliding represented by the upstroke pauses seen in the swallows, and where a particular species falls on this continuum is determined by its size, wing and muscle morphology. These characters are in turn the products of evolutionary adaptations moulded by a species' flight requirements.

### **Acknowledgements**

We are grateful to Colin J. Pennycuick for discussions and suggestions about swallow flight, and to Matthew Evans for comments on a previous draft of this manuscript. Financial support was provided by NERC grant GR3/10600 to M.R. Evans and the Swedish Natural Science Research Council and the Carl Tryggers foundation to A. H.

### **References**

- Barbosa, A. and Møller, A. P. (1999). Aerodynamic costs of long tails in male barn swallows *Hirundo rustica* and the evolution of sexual size dimorphism. *Behav. Ecol.* **10**, 128-135
- Buchanan K. L. and Evans M. R. (2000). The effect of tail streamer length on aerodynamic performance in the barn swallow. *Behav. Ecol.* **11**, 228-238.
- Danielsen, R. (1988) Bounding flight in passerines: some empirical data. *Dansk Orn. Foren. Tidsskr.* **82**, 59-60.
- Evans, M. R. (1998). Selection on swallow tail streamers. *Nature* **394**, 233-234.

- Evans, M.R. (1999). Length of tail streamers in barn swallows - reply to Hedenström & Møller. *Nature* **397**, 115-116.
- Evans, M. R. and Thomas, A. L. R. (1992). The aerodynamic and mechanical effects of elongated tails in the scarlet-tufted malachite sunbird: measuring the cost of a handicap. *Anim. Behav.* **43**, 337-347.
- Hedenström, A. and Møller, A. P. (1999). Lengths of tail streamers in barn swallows. *Nature* **397**, 115.
- Lighthill, M. J. (1977). Introduction to the scaling of aerial locomotion. In *Scale effects in animal locomotion* (ed. T. J. Pedley), pp. 365-404. London: Academic Press.
- MathSoft Inc. (2000). *S-Plus 2000 guide to statistics*, volume 2. Data Analysis Products Division, MathSoft, Seattle, WA.
- Norberg, R. Å. (1994). Swallow tail streamer is a mechanical device for self-deflection of tail leading edge, enhancing aerodynamic efficiency and flight manoeuvrability. *Proc. Roy. Soc. Lond. B* **257**, 227-233.
- Pennycuik, C. J. (1975). Mechanics of flight. In *Avian biology* (volume 5) (eds Farner, D.S. and King, J. R.), pp 1-75. London: Academic Press.
- Pennycuik, C. J. (1989a). *Bird flight performance: A practical calculation manual*. Oxford: Oxford University Press.
- Pennycuik, C. J. (1989b). Span-ratio analysis used to estimate effective lift:drag ratio in the double-crested cormorant *Phalacrocorax auritus* from field observations. *J. exp. Biol.* **142**, 1-15.
- Pennycuik, C. J. (1996). Wingbeat frequency of birds in steady cruising flight: new data and improved predictions. *J. exp. Biol.* **199**, 1613-1618.

- Pennycuik, C.J., Alerstam, T. and Hedenström, A. (1997). A new low-turbulence wind tunnel for bird flight experiments at Lund University, Sweden. *J. exp. Biol.* **200**, 1441-1449.
- Pennycuik, C.J., Hedenström, A. and Rosén, M. (2000). Horizontal flight of a swallow (*Hirundo rustica*) observed in a wind tunnel, with a new method for directly measuring mechanical power. *J. exp. Biol.* **203**, 1755-1765.
- Pennycuik, C. J., Klaassen, M., Kvist, A. and Lindström, Å. (1996). Wingbeat frequency and the body drag anomaly: wind-tunnel observations on a thrush nightingale (*Luscinia luscinia*) and a teal (*Anas crecca*). *J. exp. Biol.* **199**, 2757-2765.
- Rayner, J. M. V. (1979). A new approach to animal flight mechanics. *J. exp. Biol.* **80**, 17-54.
- Rayner, J. M. V. (1985). Bounding and undulating flight in birds. *J. theor. Biol.* **117**, 47-77.
- Rayner, J. M. V. (1995). Flight mechanics and constraints on flight performance. *Israel J. Zool.* **41**, 321-342.
- Rayner, J. M. V. (1999). Estimating power curves of flying vertebrates. *J. exp. Biol.* **202**, 3449-3461.
- Ryan, B. F., Joiner, B. I. and Ryan, T. A. (1985). *MINITAB Handbook*, 2<sup>nd</sup> edition. Boston: PWS-Kent.
- Spedding, G. R. (1987). The wake of a kestrel (*Falco tinnunculus*). *J. exp. Biol.* **127**, 59-78.
- Thomas, A. L. R. (1993). On the aerodynamics of birds' tails. *Phil. Trans. Roy. Soc. Lond. B* **340**, 361-380.
- Thomas, A. L. R. (1995). *On the tails of birds*. PhD thesis, University of Lund, Sweden.
- Thomas, A. L. R. (1996). The flight of birds that have wings and a tail: variable geometry expands the envelope of flight performance. *J. theor. Biol.* **183**, 237-245.
- Tobalske, B. W. (1995). Neuromuscular control and kinematics of intermittent flight in the European starling (*Sturnus vulgaris*). *J. exp. Biol.* **198**, 1259-1273.

- Tobalske, B. W. (1996). Scaling of muscle composition, wing morphology, and intermittent flight behavior in woodpeckers. *Auk* **113**, 151-177.
- Tobalske, B. W. and Dial, K. P. (1994). Neuromuscular control and kinematics of intermittent flight in budgerigars (*Melopsittacus undulatus*). *J. exp. Biol.* **187**, 1-18.
- Tobalske, B. W. and Dial, K. P. (1996). Flight kinematics of black-billed magpies and pigeons over a wide range of speeds. *J. exp. Biol.* **199**, 263-280.
- Tobalske, B. W., Peacock, W. L. and Dial, K. P. (1999). Kinematics of flap-bounding flight in the zebra finch over a wide range of speeds. *J. exp. Biol.* **202**, 1725-1739.
- Tucker, V. A. (1987). Gliding birds: the effect of variable wing span. *J. exp. Biol.* **133**, 33-58.

**Table 1**

Body and wing measurements for the two male barn swallows studied in the wind tunnel.

REF is a reference length on the bird from the well defined angle between the leading edge of the wing and the body to the tip of the central tail feather, used for measuring wing spans from images

	Mass	Wing span	Wing area	Aspect ratio <sup>1</sup>	REF
	(kg)	(m)	(m <sup>2</sup> )		(mm)
Swallow #1	0.0190	0.318	0.01365	7.4	94
Swallow #2	0.0180	0.328	0.01447	7.4	94

<sup>1</sup>Aspect ratio is defined as wing span squared divided by wing area

**Table 2**

Flight variable	Bird	Equation of the fitted line
Wingbeat frequency	1	$12.56 - 1.24V + 0.070V^2$
	2	$11.85 - 1.09V + 0.063V^2$
Dowstroke fraction	1	$-0.24 + 0.14V - 0.0052V^2$
	2	$-0.093 + 0.10V - 0.0029V^2$
Wingbeat amplitude (wrist)	1	$48.00 + 5.03V$
	2	$40.90 + 51.18V$
Wingspan i) mid-downstroke	1	$36.86 - 1.29V + 0.042V^2$
	2	$32.56 - 0.29V$
ii) mid-upstroke	1	$19.85 - 1.29V$
	2	$18.13 - 1.19V$
iii) span ratio	1	$0.63 - 0.039V$
	2	$0.58 - 0.037V$
Body tilt angle	1	$32.08 - 3.51V + 0.11V^2$
	2	$39.37 - 5.70V + 0.25V^2$
Tail angle of spread	1	$178.26 - 52.88V + 5.27V^2 - 0.17V^3$
	2	$213.90 - 85.63V + 13.35V^2 - 0.92V^3 + 0.024V^4$
Tail angle of attack	1	$75.97 - 18.58V + 1.63V^2 - 0.049V^3$
	2	$51.47 - 10.56V + 0.79V^2 - 0.019V^3$

## Figure legends

Fig. 1 Wingbeat frequency had a significant curvilinear relationship (quadratic function) with air speed for both birds (GLM, bird #1:  $F_{1,8} = 126.88$ ,  $P < 0.0001$ ; bird #2:  $F_{1,8} = 84.83$ ,  $P < 0.0001$ ). The equation for the fitted curve is given in Table 2. The proportion of variance ( $R^2$ ) explained by the statistical model was extremely high for both birds (96.9% and 96.1% respectively). Values are means  $\pm$  s.e.

Fig. 2 The downstroke fraction of the wingbeat cycle period. Horizontal lines represent a fraction of 0.5 where the downstroke and upstroke fractions are equal. For both birds, the relationship between downstroke fraction and air speed was best represented with a quadratic function (GLM, bird #1:  $F_{1,8} = 176.08$ ,  $P < 0.0001$ ; bird #2:  $F_{1,7} = 21.45$ ,  $P < 0.01$ ). Values are means  $\pm$  s.e.

Fig. 3 Wingbeat amplitude (A: wrist amplitude = ●, wingtip amplitude = □) increased with air speed (wrist amplitude, GLM, bird #1:  $F_{1,9} = 276.05$ ,  $P < 0.0001$ ,  $R^2 = 96.5\%$ ; bird #2:  $F_{1,8} = 241.85$ ,  $P < 0.0001$ ,  $R^2 = 96.4\%$ ). The duration of the downstroke (B) decreased, and the downstroke angular velocity (C) increased with air speeds exceeding  $7 \text{ ms}^{-1}$ . Values are means  $\pm$  s.e.

Fig. 4 Mid-downstroke (maximum) wingspan (A) decreased with increasing air speed, although for bird #1 this relationship was best represented with a quadratic function and for bird #2, a linear function (GLM, bird #1:  $F_{1,8} = 12.54$ ,  $P < 0.01$ ,  $R^2 = 85.9\%$ ; bird #2:  $F_{1,8} = 63.42$ ,  $P < 0.0001$ ,  $R^2 = 88.8\%$ ). Mid-upstroke (minimum) wingspan (GLM, bird #1:  $F_{1,9} = 73.37$ ,  $P < 0.0001$ ,  $R^2 = 89.1\%$ ; bird #2:  $F_{1,8} = 91.09$ ,  $P < 0.0001$ ,  $R^2 = 91.9\%$ ; Fig. 4B) and wingspan ratio (GLM, bird #1:  $F_{1,9} = 67.61$ ,  $P < 0.0001$ ,  $R^2 = 88.3\%$ ; bird #2:  $F_{1,8} = 86.72$ ,  $P$

$< 0.0001$ ,  $R^2 = 91.6\%$ ; Fig. 4C) also decreased with increasing air speed. Values are means  $\pm$  s.e.

Fig. 5 A brief pause was observed during the upstroke at air speeds exceeding  $6 \text{ ms}^{-1}$  (A) and  $8 \text{ ms}^{-1}$  (B). The average length of these pauses at each air speed has been calculated using only those wingbeats containing the pauses (i.e. does not include pauses of zero length). The duration of these pauses reached maximal levels between  $10\text{-}12 \text{ ms}^{-1}$ . Values are means  $\pm$  s.e.

Fig. 6 Wingtip path of a characteristic wingbeat in lateral view (A) and rear view (B) at  $4 \text{ ms}^{-1}$ ,  $8 \text{ ms}^{-1}$  and  $12 \text{ ms}^{-1}$ . Arrows indicate the direction of movement and filled circles indicate the position of the wingtip on each frame with  $8 \text{ ms}$  between nearest circles. The silhouettes illustrate the body posture at the upstroke/downstroke transition.

Fig. 7 Body tilt averaged across the upstroke, downstroke and mid-stroke portions of the wingbeat cycle. For both birds, body tilt angle had a significant quadratic relationship with air speed, and decreased with increasing air speed (GLM, bird #1:  $F_{1,8} = 5.92$ ,  $P < 0.05$ ; bird #2:  $F_{1,7} = 41.78$ ,  $P < 0.0001$ ). Values are means  $\pm$  s.e.

Fig. 8 Tail spread (A) decreased with increasing air speed, although for bird #1 this relationship was best represented by a cubic function, and for bird #2 a quartic function (GLM, bird #1:  $F_{1,7} = 17.61$ ,  $P < 0.01$ ; bird #2:  $F_{1,5} = 13.05$ ,  $P < 0.05$ ). Tail angle of attack (B) also decreased with increasing air speed, and for both birds this relationship was best represented by a cubic function (GLM, bird #1:  $F_{1,7} = 8.36$ ,  $P < 0.05$ ; bird #2:  $F_{1,6} = 6.42$ ,  $P < 0.05$ ). The angle of tail spread in some of the flight sequences for bird #1 (Fig. A i) were

obsured: the number of flight sequences for which tail spread angle data were obtained, therefore, varies between one and five. All other  $n = 5$ . Values are means  $\pm$  s.e.

Fig. 1

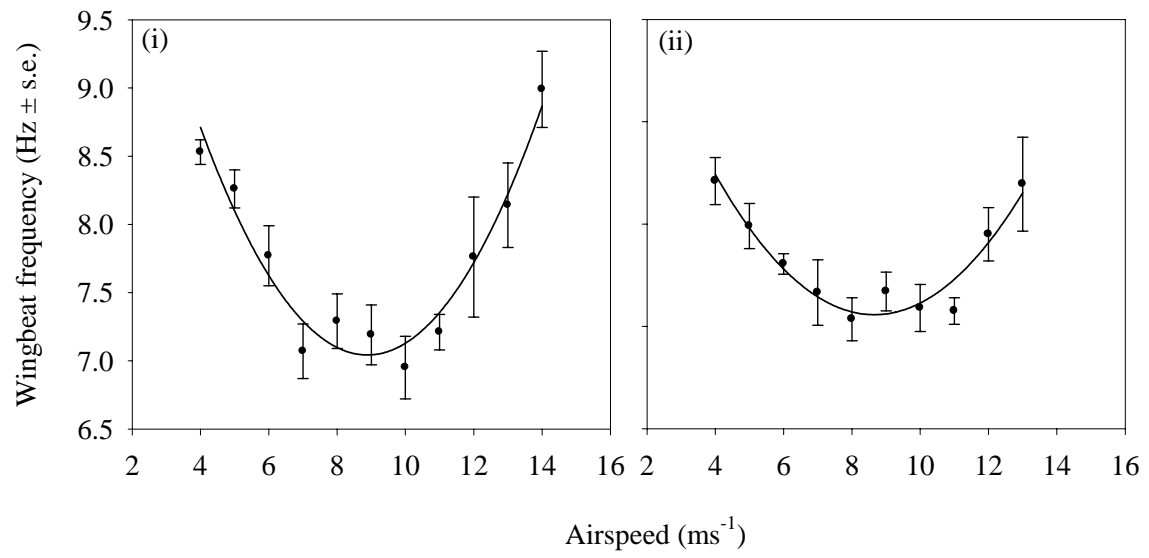


Fig. 2

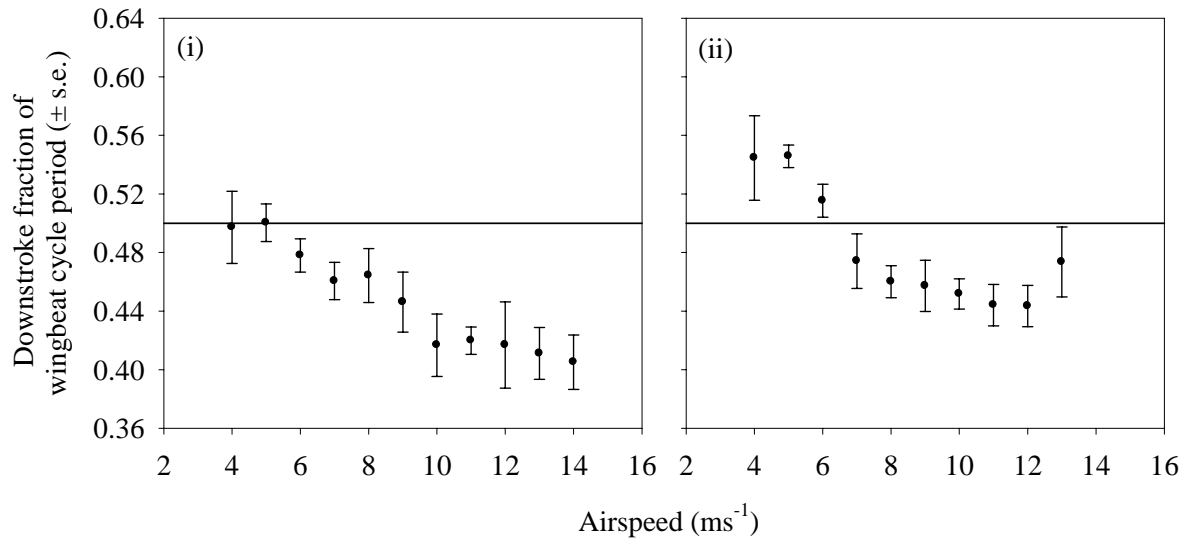


Fig. 3

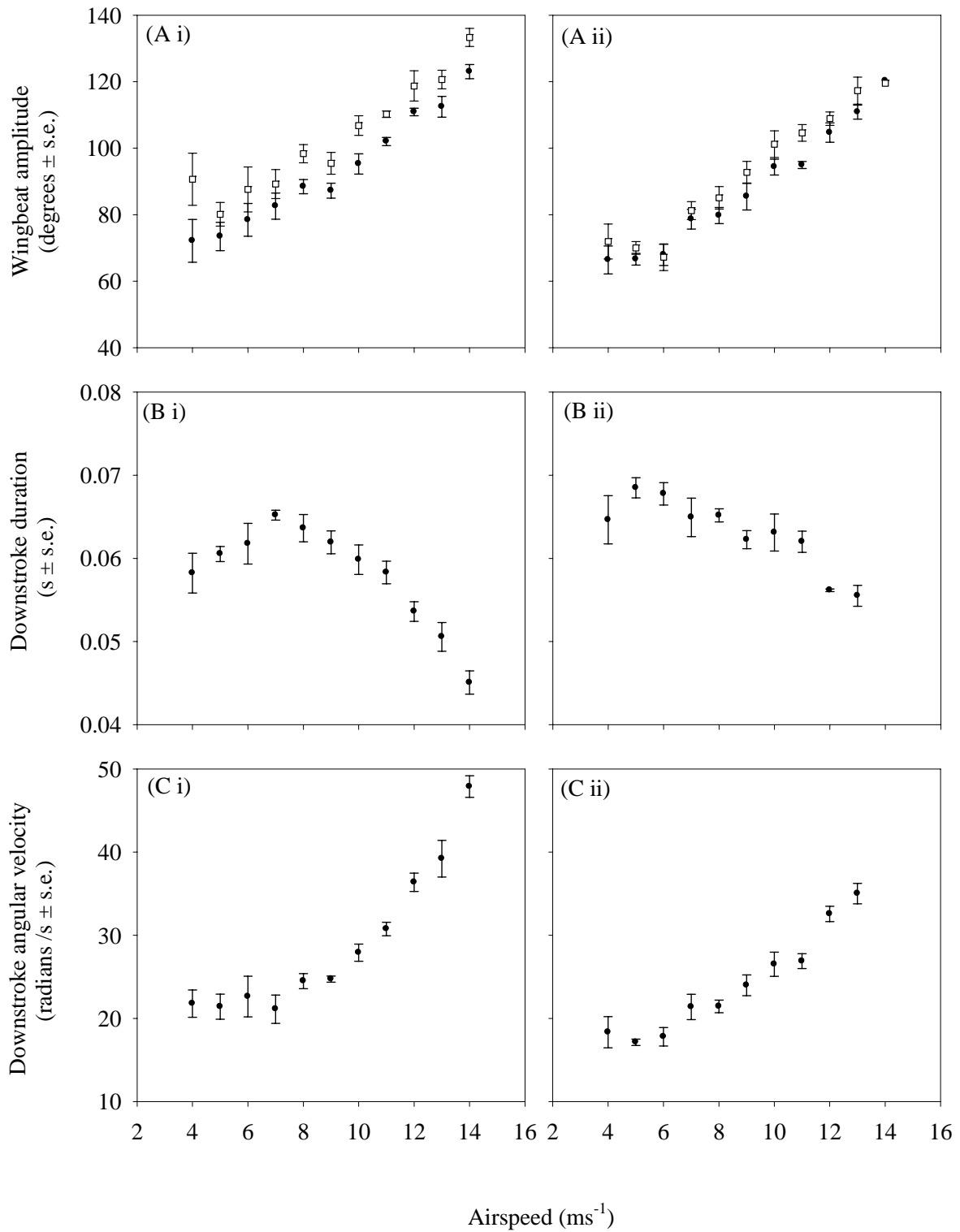


Fig. 4

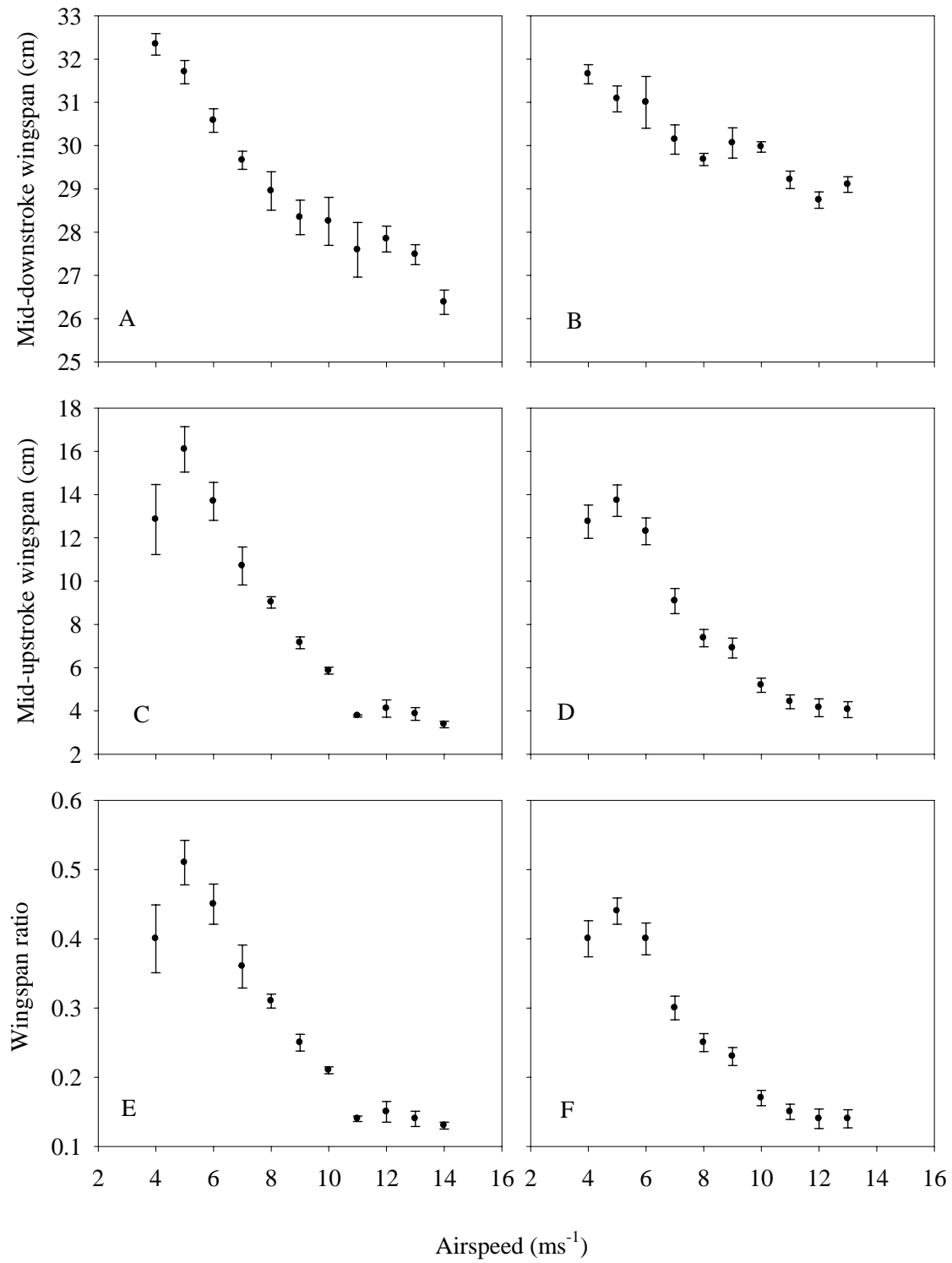


Fig. 5

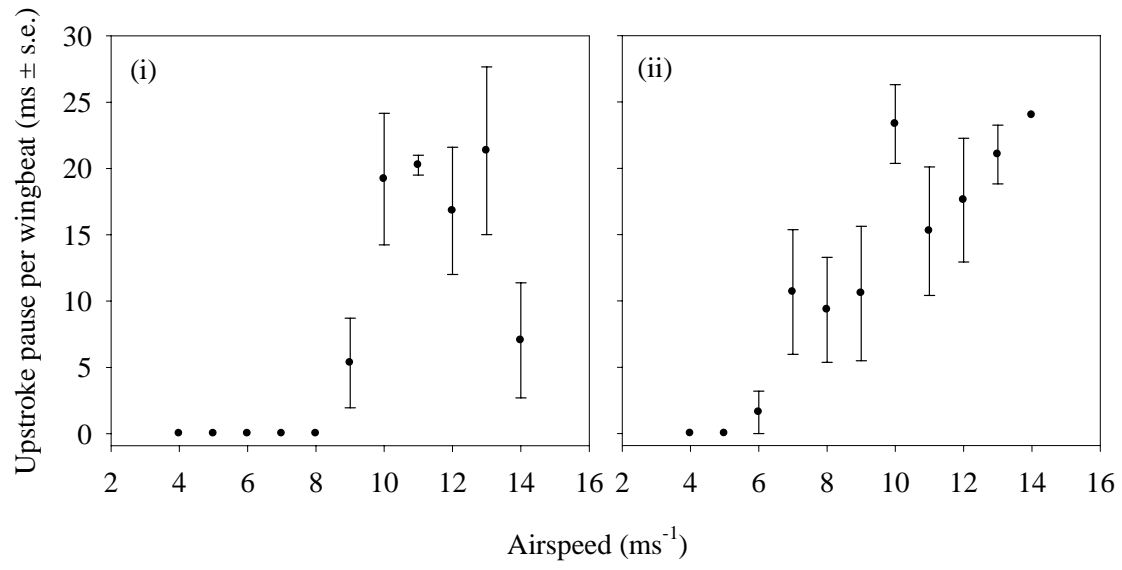


Fig. 6

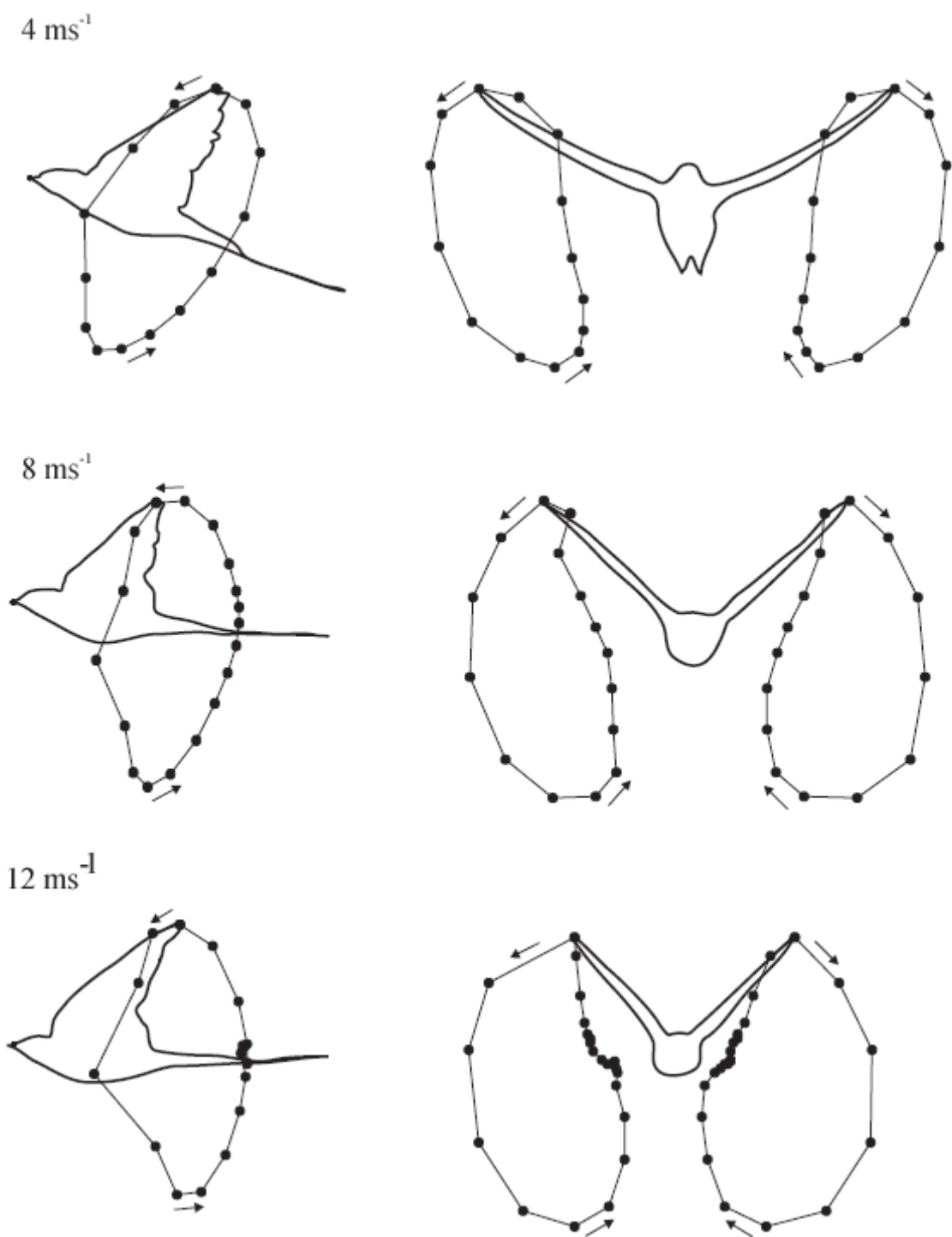


Fig. 7

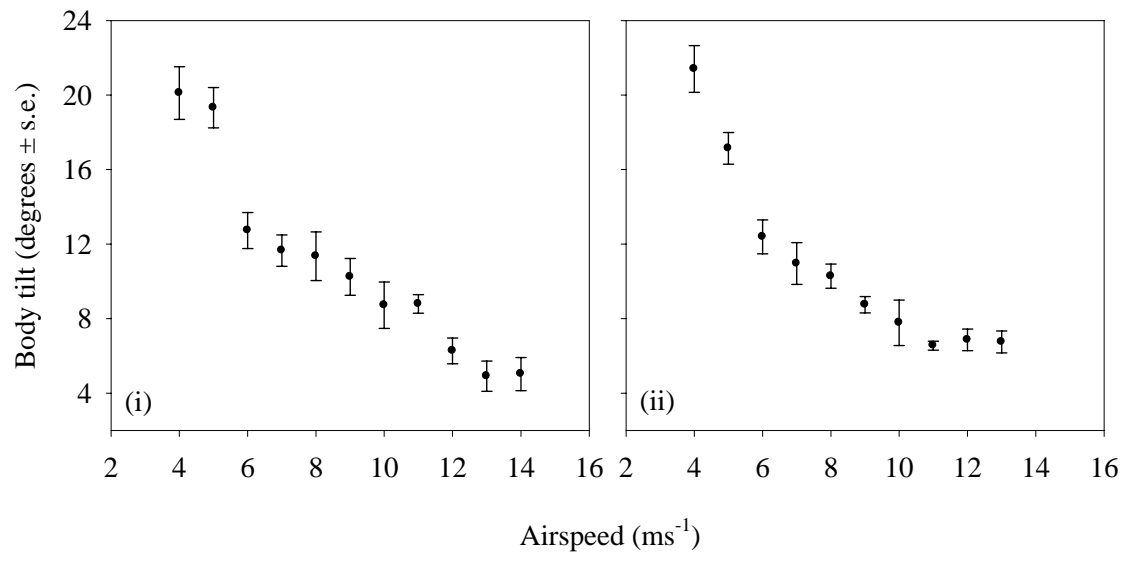


Fig. 8

